

Structural and Electrical Properties of $\text{Li}_{4.08+x}\text{Zn}_{0.04}\text{Al}_x\text{Si}_{0.96-x}\text{O}_4$ Ceramic Electrolyte

Syed Bahari Ramadzan Syed Adnan* and Nor Sabirin Binti Mohamed

Centre for Foundation Studies in Science, University of Malaya, 50603 Kuala Lumpur, Malaysia

*syed_bahari@um.edu.my

(Received: 1 June 2016; published 17 July 2016)

Abstract. In this paper, we report the effect of Al^{3+} substitutions to the structural and electrical properties of $\text{Li}_{4.08}\text{Zn}_{0.4}\text{Si}_{0.96}\text{O}_4$ ceramic electrolyte. X-ray diffraction was applied to study the structural properties such as crystalline phase, lattice parameter and unit cell volume of the solid electrolytes. The electrical properties of the compounds measured by AC impedance as a function of frequency in the range between 0.1 Hz to 10 MHz and in a temperature range between 473 K to 773 K. The optimal value of the total conductivity was reached at $x = 0.03$ measured at 773 K. This result indicates that the substitutions of Al^{3+} in the $\text{Li}_{4.08}\text{Zn}_{0.4}\text{SiO}_4$ structure, improved the conductivity due to the enhancement of Li^+ ion concentration and mobility.

Keywords: Ceramic, Ionic Conductivity, Lithium Orthosilicate, Solid electrolyte.

I. INTRODUCTION

Safety and reliability are the most important points in next-generation battery systems that will be developed in our bright and clean-energy future society. It is believed that all-solid-state batteries using ceramic solid electrolytes are one of the ultimate goals of rechargeable energy sources for future vehicles and energy storage systems. Single cation conduction and no solvation of carrier ions in ceramic solid electrolytes, which result in less side reactions and wide electrochemical windows, will provide us with an ideal battery system with a high level of safety and reliability. Meanwhile the ceramic electrolytes also can be used with active materials with higher capacity, such as metallic lithium and elemental sulfur, which are difficult to use in an organic liquid electrolyte cell [1].

Basically, ceramic materials consist of lattice and basis which represent as a crystal structure [2]. Lattice structure will act as a migration tunnel in the ceramic structure to allow the movement of the cation. Inorganic crystalline electrolytes or ceramic electrolytes are the only solid electrolytes that have ordered structure. They basically consist of mobile ions in less or more rigid crystalline frameworks. The ionic conduction in the crystalline electrolytes is through 1D, 2D or 3D channels depending on the crystal structure. Ionic conduction in this electrolyte occurs by movement of ionic point defects which requires energy in their periodic lattice structure. These point defects produce interstitial or vacant ions that can enhance the mobility of ions and ionic conductivity as well [3-4].

It is known that modification of the lattice size has been made widely in order to enhance the conductivity of the sample. For example, the partial substitution of Si^{4+} by $\text{M} = \text{B}^{3+}, \text{Al}^{3+}, \text{Ga}^{3+}, \text{Cr}^{3+}$ and Fe^{3+} ions have been done on Lisicon-type network structure of Li_4SiO_4 compound with the formula of $\text{Li}_{4+x}\text{M}_x\text{Si}_{1-x}\text{O}_4$ [5-9]. Meanwhile, the study of $\text{Li}_{4.08}\text{Zn}_{0.04}\text{Si}_{0.96}\text{O}_4$ compound which is based on partial substitution of Zn^{2+} with Si^{4+} ($2\text{Li}^+ + \text{Zn}^{2+} \leftrightarrow \text{Si}^{4+}$) in the $\text{Li}_{4+2x}\text{Zn}_x\text{Si}_{1-x}\text{O}_4$ ($x=0.04$) system has been reported by the authors recently [9-10]. Apart from enlarging the migration tunnel in the structure due to the larger size of Zn^{2+} than Si^{4+} , the substituted of Zn^{2+} in the Li_4SiO_4 lattice structure also introduces two interstitial ions which are expected to enhance the mobile ion concentration and leading to increase the conductivity.

In the present work, we expect to enhance the conductivity of $\text{Li}_{4.08}\text{Zn}_{0.04}\text{Si}_{0.96}\text{O}_4$ by partial substituted Al^{3+} with the Si^{4+} ($\text{Li}^+ + \text{Al}^{3+} \leftrightarrow \text{Si}^{4+}$) with the formula of $\text{Li}_{4.08+x}\text{Zn}_{0.04}\text{Al}_x\text{Si}_{0.96-x}\text{O}_4$. To the best of our knowledge, limited studies have been carried out using Al^{3+} as the property enhancing agent in the $\text{Li}_{4.08}\text{Zn}_{0.04}\text{Si}_{0.96}\text{O}_4$ structure. So, for the first time, detail structure and electrical properties of $\text{Li}_{4.08+x}\text{Zn}_{0.04}\text{Al}_x\text{Si}_{0.96-x}\text{O}_4$ is reported.

II. EXPERIMENTAL PROCEDURE

A. Synthesis of samples

For preparation of the sample, lithium acetate, zinc acetate, aluminium acetate and tetraethyl orthosilicate were used as the starting materials while citrate acid was used as the chelating agent. All the chemicals were first dissolved in distilled water with a molar ratio of $\text{Li} : \text{Zn} : \text{Al} : \text{Si}$ fixed according to formula $\text{Li}_{4.08+x}\text{Zn}_{0.04}\text{Al}_x\text{Si}_{0.96-x}\text{O}_4$ ($x = 0.01, 0.02, 0.03$). Solution of citrate acid was mixed together with the previously prepared chemical solutions under magnetic stirring. The solutions were transferred into reflux systems and continuously stirred until homogeneous solutions were formed. Solution of tetraethyl orthosilicate was later added to these homogeneous solutions. After stirring for 12 hours, the solutions were taken out and then vaporized for about 2 hours under magnetic stirring at 75°C . The resulting sticky wet gels formed were dried in an oven at 150°C for 24 hours. The powders were sintered at temperature 800°C for 12 hours and later pressed using a Specac hydraulic pellet press to form pellets with diameter and thickness of 13 mm and 2.0 mm.

B. Characterization techniques

X-ray diffraction (XRD) was done in order to elucidate structural information of the synthesized ceramic samples. XRD patterns of the powder samples were obtained using X-ray Diffraction spectrometer PANalytical-X'pert³ with Cu-K_α radiation of wavelength of 1.5406 \AA in 2θ range between 10° to 70° at the rate of 0.016° in step width. The data obtained were analyzed using High score plus software. The lattice parameters of the monoclinic compound were calculated using equation as follows [8],

$$\frac{1}{d^2} = \frac{1}{\sin^2 \beta} \left(\frac{h^2}{a^2} + \frac{k^2 \sin^2 \beta}{b^2} + \frac{l^2}{c^2} \right) - \frac{2hl \cos \beta}{ac}, \quad d = \frac{\lambda}{2 \sin \theta} \quad (1)$$

where d is the distance between crystal planes of (hkl) , λ is the X-ray wavelength, θ is the diffraction angle of a crystal plane (hkl) , hkl is the crystal index, a , b and c are the lattice parameters and β is the angle between a and c (90.25°). The morphology of the sample powders were analyzed by scanning electron microscope (SEM) which were carried out using Zeiss Evo MA10. The ceramic electrical properties were determined by alternate current (AC) impedance spectroscopy which was performed using Solatron 1260 impedance analyzer over a frequency range from 0.1 to 10 MHz. An applied voltage was fixed at 200 mV. The total conductivity, σ_t (bulk conductivity, σ_b + grain boundary conductivity, σ_{gb}) which represents the direct current (DC) conductivity in the ceramic sample was calculated using the equation [8,11] :

$$\frac{1}{\sigma_t} = \frac{1}{\sigma_b} + \frac{1}{\sigma_{gb}} \quad (2)$$

where $\sigma_b = \frac{d}{AR_b}$ and $\sigma_{gb} = \frac{d}{AR_{gb}}$

In these equations, d is the sample thickness, A is the cross-sectional area of the sample, R_b is the bulk resistance and R_{gb} is the grain boundary resistance.

III. RESULTS AND DISCUSSIONS

Fig. 1 shows the XRD patterns of the $\text{Li}_{4.08+x}\text{Zn}_{0.04}\text{Al}_x\text{Si}_{0.96-x}\text{O}_4$ ($x = 0.01, 0.02, 0.03$) ceramic electrolytes with various Al contents.

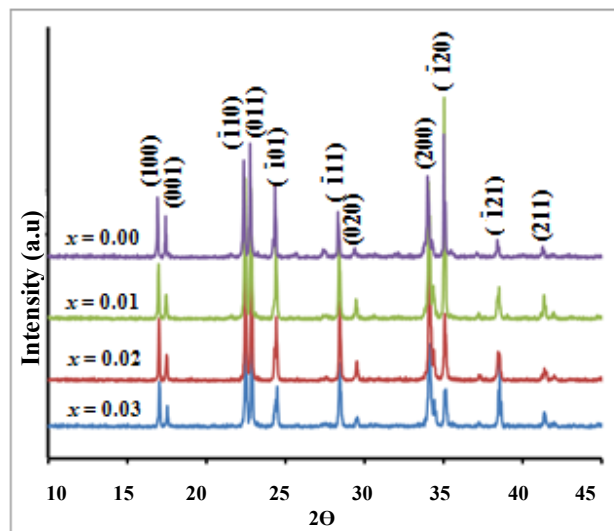


FIGURE 1. XRD patterns of $\text{Li}_{4.08+x}\text{Zn}_{0.04}\text{Al}_x\text{Si}_{0.96-x}\text{O}_4$ samples

All patterns show a single phase with a monoclinic structure and no secondary phase, suggesting that Al^{3+} ions can be well substituted into the lithium zinc orthosilicate lattice. From equation (1), when the Al content was increased up to 0.03, the peaks at (100),(020) and (001) planes which represent lattice parameters of a , b and c respectively were shifted. The 2Θ value peak at (100) and (020) shifted slightly towards the upper degree because the value of d was decreased; on the other hand, the 2Θ value peak at (001) shifted slightly towards the lower degree because the value of d was increased. The correlation between the lattice parameters and unit cell volume ($V = abc \sin \beta$) with the various contents of Al is shown in Fig. 2. As shown, the unit cell volume linearly increased with increasing Al content because the ionic radius of Al^{3+} (0.54 Å) is larger than that of Si^{4+} (0.41 Å). Meanwhile, this also may attribute to the extra lithium ion content in the structure. As a result of above, it was confirmed that Si^{4+} has be substituted with Al^{3+} in $\text{Li}_{4.08}\text{Zn}_{0.4}\text{Si}_{0.96}\text{O}_4$ lattice structure.

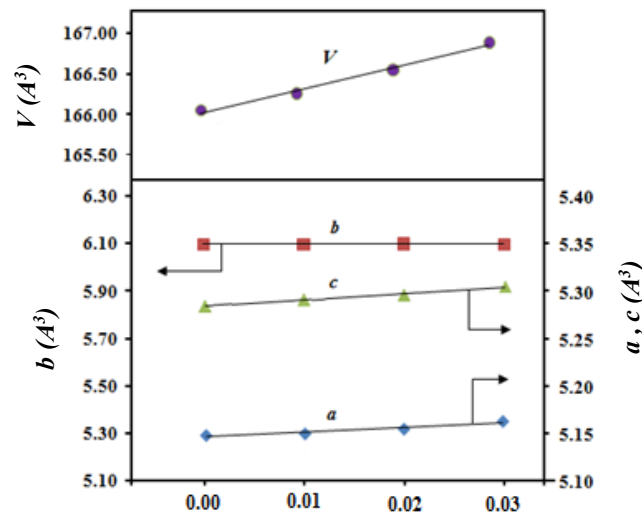


FIGURE 2. Lattice parameters and unit cell volume of $\text{Li}_{4.08+x}\text{Zn}_{0.04}\text{Al}_x\text{Si}_{0.96-x}\text{O}_4$ samples

The surface micro- structures of the $\text{Li}_{4.08+x}\text{Zn}_{0.04}\text{Al}_x\text{Si}_{0.96-x}\text{O}_4$ ceramic electrolytes sintered at the 800°C with various Al contents are shown in Fig.3. The grain size of the sample $x = 0.01$ (average $8.2 \mu\text{m}$) is smaller than those of the other samples. When the Al contents were increased up to 0.03, the grain sizes of the samples gradually increased. The grain size of the $\text{Li}_{4.08+x}\text{Zn}_{0.04}\text{Al}_x\text{Si}_{0.96-x}\text{O}_4$ ceramics at $x = 0.03$ were greater than those of the other samples with the average size of $14.3 \mu\text{m}$.

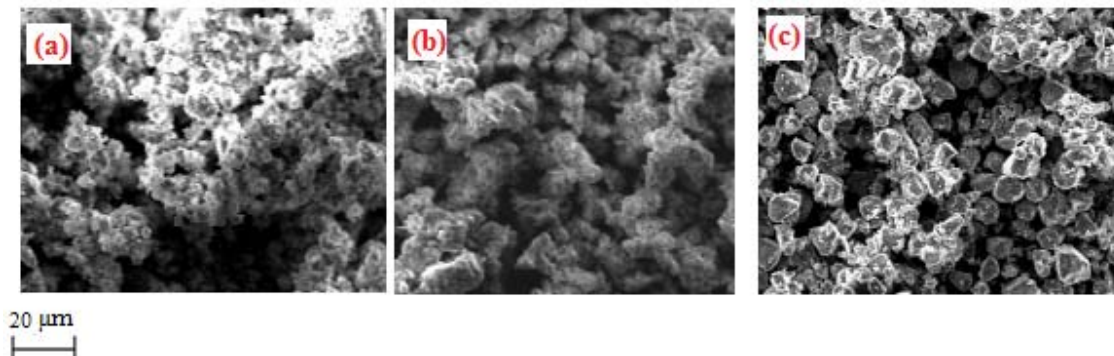


FIGURE 3. Surface micrograph of $\text{Li}_{4.08+x}\text{Zn}_{0.04}\text{AlSi}_{0.96-x}\text{O}_4$ samples with various Al contents; (a) 0.01 (b) 0.02 (c) 0.03

Typical complex impedance spectra for $\text{Li}_{4.08+x}\text{Zn}_{0.04}\text{Al}_x\text{Si}_{0.96-x}\text{O}_4$ ($0.01 \leq x \leq 0.03$) compounds at 473 K are shown in Fig.4. The spectra consist of two depressed semicircles in high and intermediate frequency region followed by a spike in the low frequency region. The depressed semicircles at high frequency and intermediate frequency are due to bulk resistance (R_b) and grain boundary resistance (R_{gb}) of the compound. Meanwhile, the spike in the low frequency is due to the processes occurring at the electrode and electrolyte interface [12]. As the substitution of Al content increase, the total resistance, $R_t = (R_b + R_{gb})$ value shifts towards a lower value indicating an increase in conductivity. The σ_b , σ_{gb} and σ_t values of $\text{Li}_{4.08+x}\text{Zn}_{0.04}\text{Al}_x\text{Si}_{0.96-x}\text{O}_4$ ($0.01 \leq x \leq 0.03$) compounds at 473 K are listed in Table 1.

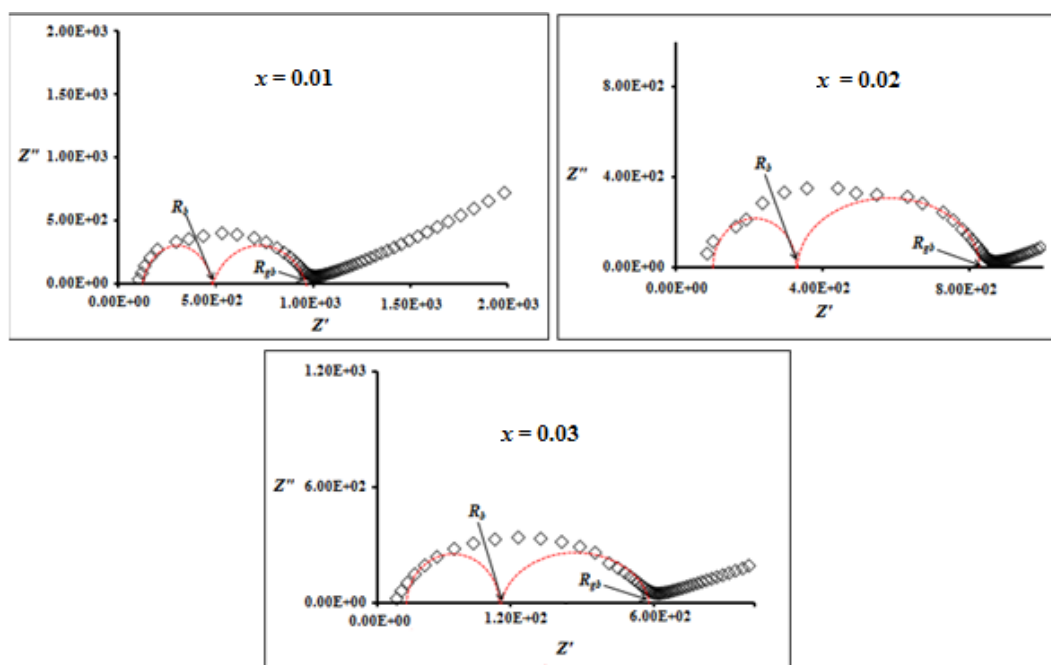


FIGURE 4. Typical complex impedance spectra for $\text{Li}_{4.08+x}\text{Zn}_{0.04}\text{Al}_x\text{Si}_{0.96-x}\text{O}_4$ ($0.01 \leq x \leq 0.03$) compounds at 473 K

The semicircles observed in the graphs also can be represented by the equivalent circuit using a combination of resistance R_p and capacitance, C_p with the constant phase element (CPE) behavior. A CPE is equivalent to a distribution of capacitor in parallel where were calculated from the observed impedance spectra using the circuit shown in Fig.5. The general expression of the CPE is [13] ;

$$Z = \frac{1}{C(j\omega)^n} \tag{3}$$

Here, C indicates ideal capacitance where $n = 1, j = (-1)^{1/2}$ and ω shows the angular frequency. The equivalent circuit consists of a series of array of parallel RC elements attached with a series resistor, R_s . Series resistance corresponds to bulk resistance, whereas grain boundary resistance is represented by a resistance which attaches in parallel to a capacitor [14].

TABLE 1. The σ_b , σ_{gb} and σ_t values of $\text{Li}_{4.08+x}\text{Zn}_{0.04}\text{Al}_x\text{Si}_{0.96-x}\text{O}_4$ ($0.01 \leq x \leq 0.03$) compounds at 473 K

Samples	$\sigma_b (S\text{ cm}^{-1})$	$\sigma_{gb} (S\text{ cm}^{-1})$	$\sigma_t (S\text{ cm}^{-1})$
$x = 0.01$	4.13×10^{-4}	2.37×10^{-4}	1.51×10^{-4}
$x = 0.02$	5.09×10^{-4}	2.73×10^{-4}	1.79×10^{-4}
$x = 0.03$	1.26×10^{-3}	2.10×10^{-4}	2.51×10^{-4}

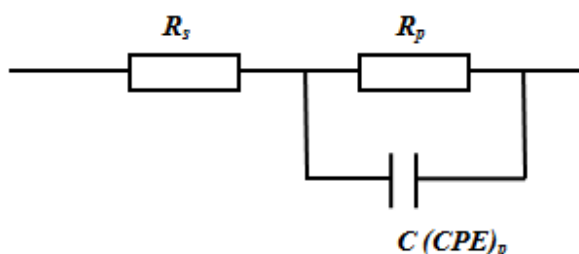


FIGURE 5. Equivalent circuit of the samples on the basis of impedance analysis

Figure 6 presents the relationship between total conductivity of $\text{Li}_{4.08+x}\text{Zn}_{0.04}\text{Al}_x\text{Si}_{0.96-x}\text{O}_4$ ($0.01 \leq x \leq 0.03$) with temperature. The total conductivities fit the Arrhenius equation:

$$\sigma_t T = A(T) \exp\left(\frac{-E_a}{kT}\right) \tag{4}$$

where A is the pre-exponential factor, E_a is the activation energy for conduction and k is the Boltzman constant. The $\text{Li}_{4.08+x}\text{Zn}_{0.04}\text{Al}_x\text{Si}_{0.96-x}\text{O}_4$ with $y = 0.03$ shows the highest total conductivity of $2.51 \times 10^{-4} \text{ S cm}^{-1}$ at 473 K and $1.78 \times 10^{-3} \text{ S cm}^{-1}$ at 773K. This value is an order of magnitude higher compared to the parent compound reported earlier by the authors [14]. The linear relationships are observed for the whole testing temperature range, suggesting that there are no structural and phase changes in the samples. The activation energy of the samples

was extracted from the slope of the Arrhenius graph and also shown in Figure 6. The low activation energy indicates an easier movement of lithium ion from one site to another in the lattice structure which resulting high mobility of ions and conductivity as well.

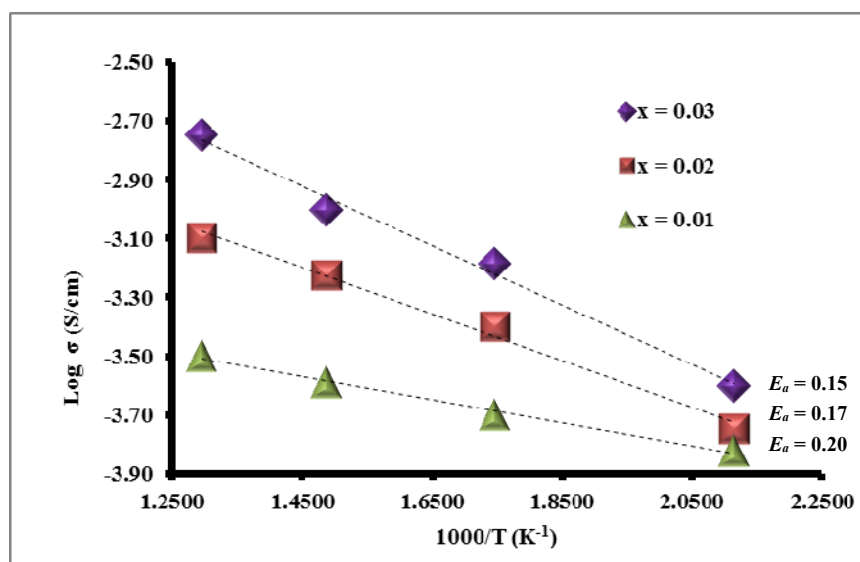


FIGURE 6. Temperature dependence of total conductivity for $\text{Li}_{4.08+x}\text{Zn}_{0.04}\text{Al}_x\text{Si}_{0.96-x}\text{O}_4$ samples

IV. CONCLUSIONS

The effect of Al substitutions on the $\text{Li}_{4.08+x}\text{Zn}_{0.04}\text{Al}_x\text{Si}_{0.96-x}\text{O}_4$ ($0.01 \leq x \leq 0.03$) compounds was investigated by X-ray diffraction and impedance spectroscopy. The XRD result indicated that Zn^{2+} and Al^{3+} were successfully inserted into the Li_4SiO_4 structure. The compound with $x = 0.03$ showed the highest conductivity value (an order of magnitude higher than that of the parent compound) due to the presence of extra interstitial Li^+ ions that contributed to conductivity and their enhanced mobility.

Acknowledgements

The authors great fully acknowledge the financial support from the University of Malaya in the form of research grants (grant no. BK049-2014) for this research project.

1. M. Tatsumisago, R. Takano, K. Tadanaga, *Journal of Power Sources* **270**, 603–607 (2014)
2. A.R West, *Solid State Chemistry and its Applications*, John Wiley and Sons Ltd, New York, 1984 pp 28-35.

3. J.W Fergus, *Journal of Power Sources* **162**, 30-40 (2006).
4. J.W Fergus, *Journal of Power Sources* **195**, 4554-4569 (2010).
5. C. Masquelier, M. Tabuchi, T. Takeuchi, W. Soizumi, H. Kageyama, O. Nakamura, *Solid State Ionics* **79**, 98 -105 (1995).
6. Y. Saito, K. Ado, T. Asai, H. Kageyama, O. Nakamura, *Solid State Ionics* **47**, 149-154 (1991).
7. Y. Saito, T. Asai, K. Ado, H. Kagayema, O. Nakamura, *Solid State Ionics* **40-41**, 34-37(1990).
8. S.B.R.S Adnan, N.S Mohamed, *Electrochimica Acta* **146**, 598-610 (2014).
9. S.B.R.S Adnan, N.S Mohamed, *Materials Characterization* **96**, 249-255 (2014).
10. S.B.R.S Adnan, N.S Mohamed, *Ionics* **20**, 1641-1650 (2014).
11. S.R. Hui, J. Roller, S. Yick, X. Zhang, C. Decès-Petit, Y. Xie, R. Maric, D. Ghosh, *Journal of Power Sources* **172**, 493-502 (2007).
12. P. Ferloni and A. Magistris, *Journal de Physique* **IV**, C1-3 – C1-15 (1994).
13. D.F. Zhou, Y.J. Xia, J.X. Zhu, J. Meng, *Solid State Sciences* **11**, 1587-1591 (2009).
14. P. Yadav, M.C Bhtnagar, *Ceramics International* **38**, 1731-1735 (2012).
15. S.B.R.S Adnan, N.S. Mohamed, *Ceramics International* **40**, 5033-5038 (2014).